THE ASTROPHYSICAL JOURNAL, 340:537–549, 1989 May 1

INFRARED EMISSION FROM COMETS

K. S. KRISHNA SWAMY,[1] S. A. SANDFORD, L. J. ALLAMANDOLA, F. C. WITTEBORN, AND J. D. BREGMAN
NASA/Ames Research Center, Moffett Field, California
Received 1988 February 26; accepted 1988 October 12

ABSTRACT

A brief discussion of the infrared observations from 4 to 20 μm of seven comets is presented. The observed infrared emission from comets depends primarily on their heliocentric distance. A model based on grain populations composed of a mixture of silicate and amorphous carbon particles in the mass ratio of about 40 to 1, with a power-law size distribution similar to that inferred for comet Halley, is applied to the observations. The model provides a good match to the observed heliocentric variation of both the 10 μm feature and the overall thermal emission from comets West and Halley. Matches to the observations of comet IRAS-Araki-Alcock and the antitail of comet Kohoutek require slightly larger grains. While the model does not match the exact profile and position of the 3.4 μm feature discovered in comet Halley, it does produce a qualitative fit to the observed variation of the feature's strength as a function of heliocentric distance. The calculations predict that the continuum under the 3.4 μm feature is due primarily to thermal emission from the comet dust when the comet is close to the Sun and to scattered solar radiation at large heliocentric distances, as is observed. A brief discussion of the determination of cometary grain temperatures from the observed infrared emission is presented. It is found that the observed shape of the emission curve from about 4 to 8 μm provides the best spectral region for estimating the cometary grain temperature distribution.

Subject headings: comets — infrared: spectra — spectrophotometry

I. INTRODUCTION

The infrared measurements of comet Ikeya-Seki in the 1–10 μm wavelength region showed, for the first time, that comets produce excess emission over and above the expected flux due to a scattered solar continuum (Becklin and Westphal 1966). Since then, a large number of comets have been observed, and they all show excess emission in the 2–20 μm region (see Ney 1982). The observed infrared radiation is generally attributed to thermal emission from dust grains which are heated by incident solar radiation (Krishna Swamy and Donn 1968; Krishna Swamy 1986). The nature and composition of the grain material giving rise to the observed infrared radiation is still uncertain, although the infrared measurements provide an important clue to the nature of the grain material. A broad emission feature around 10 μm, first detected in comet Bennett (Maas, Ney, and Woolf 1970), is generally attributed to Si-O stretching vibrations in some form of silicate material. Laboratory measurements show that, in general, silicates have an additional feature or features around 20 μm produced by Si-O-Si bending vibrations, and such a feature has been observed in several comets as well (Ney 1982).

Figure 1 shows the infrared spectra of a number of comets in the 4.5–20 μm wavelength region. The top two sets of spectra correspond to different comets at roughly the same heliocentric distances. The observed spectral profiles of different comets having similar solar distances agree reasonably well with one another. This general behavior appears to be valid for a wide range of heliocentric distances, implying that the shape of the emission curve produced by comets depends largely on their distance from the Sun.

Observations of the 10 μm feature in the spectra of comets show that the apparent strength of this feature varies from comet to comet, as well as with heliocentric distance for the same comet. In some cases, the 10 μm feature does not appear to be present (see Ney 1982). To date, broad-band observations of the 10 μm feature seem to indicate an *apparent* absence of this feature at heliocentric distances ≥ 1.2 AU (see Ney 1982; Hanner 1986). However, moderate-resolution spectra taken when comet Halley was at a heliocentric distance of 1.3 AU show a distinct 10 μm feature (Bregman *et al.* 1987), suggesting that the apparent absence of a silicate feature at large solar distances may be more of an observational effect than a real one.

It is interesting to note that Bregman *et al.* (1987) obtained data on 1985 December 12 and 1986 April 8, dates which correspond to pre- and postperihelion positions of the comet having roughly the same heliocentric distance. Remarkably, the 5–10 μm spectra from these two observations agree very well (Fig. 1*c*). This implies that the properties of the dominant grain materials were nearly the same on both dates.

Since different silicate minerals produce 10 μm Si-O stretching features with different band profiles, the observed shape of the 10 μm feature in comets should provide information about the composition of the grains. Unfortunately, the profile of the feature in cometary spectra was not well determined until the recent 8–13 μm observations of comet Halley by Bregman *et al.* (1987). Bouchet *et al.* (1987) have also obtained 8–13 μm spectra of comet Halley, although the errors in their observations are larger (the error bars on the Bregman *et al.* data in Fig. 1 are about the size of the points). Finally, Campins and Ryan (1988) have also obtained an 8–13 μm profile from comet Halley. All three sets of data show the same general shape of the 10 μm feature. The presence of substructure in the 10 μm feature indicates that the band is produced by crystalline silicates, not amorphous silicates (Sandford and Walker 1985; Bregman *et al.* 1987).

Comet Halley was unique in that it was extensively observed over a wide range of wavelengths and heliocentric distances (cf.

[1] NAS–NRC–NASA Research Associate on leave from the Tata Institute of Fundamental Research, Bombay, India.

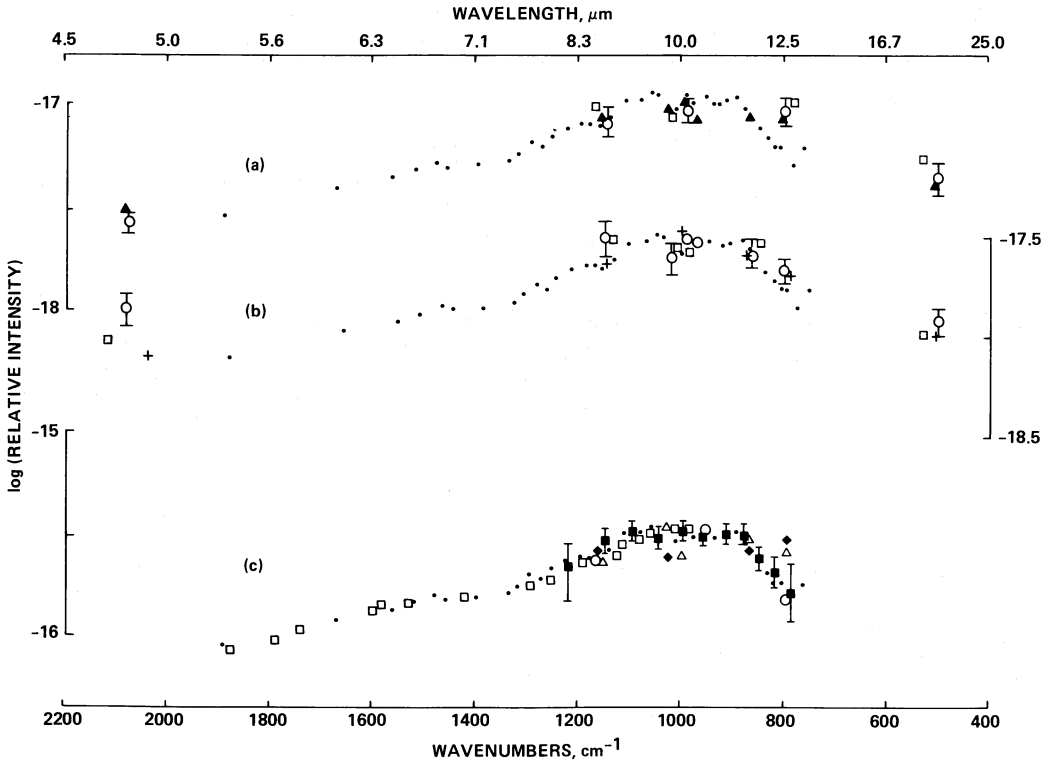

FIG. 1.—Observed 4.5–20 μm emission from several comets. (*a*) *Solid dots*: Halley, $r = 1.32$ AU, 1986 December 12, 17 (Bregman *et al.* 1987); *open squares*: Halley, $r = 1.66$ AU (Green *et al.* 1986); *open circles*: Stephan-Oterma, $r = 1.58$ AU (Hanner *et al.* 1984); *filled triangles*: Churyumov-Gerasimenko, $r = 1.35$ AU (Hanner *et al.* 1985*b*). (*b*) *Solid dots*: same as in (*a*); *open circles*: Grigg-Skjellerup, $r = 1.15$ AU (Hanner *et al.* 1984); *plus signs*: Halley, $r = 1.12$ AU (Gehrz and Ney 1986); *open squares*: Halley, $r = 1.16$ AU (Green *et al.* 1986). (*c*) All observations for comet Halley. *Solid dots*: same as in (*a*); *open squares*: $r = 1.32$ AU, 1986 April 8 (Bregman *et al.* 1987); *open triangles*: $r = 1.8$ AU (Green *et al.* 1986); *filled squares*: $r = 0.67$ AU (Bouchet *et al.* 1987); *open circles*: $r = 0.59$ AU (Gehrz and Ney 1986); *filled diamonds*: $r = 1.66$ AU (Green *et al.* 1986).

Proceedings of the 20th ESLAB Symposium on the Exploration of Halley's Comet [1986] and the special comet Halley issue of *Astronomy and Astrophysics*, Vol. **187** [1987]). As a result of this increased spectral coverage, a new broad emission feature near 3.4 μm was discovered (Combes *et al.* 1986; Wickramasinghe and Allen 1986; Danks *et al.* 1987; Baas, Geballe, and Walther 1986; Knacke, Brooke, and Joyce 1986). The position of this feature is characteristic of the C-H stretching band in hydrocarbons.

Taken together, the infrared spectra of comet Halley suggest that there are two major components in the refractory grain mixture—silicates and some form of hydrogenated carbon. Such a mixture is consistent with the compositional information available from the Halley flybys (Kissel *et al.* 1986) and from analyses of interplanetary dust particles (IDPs) (Sandford 1987). Earlier work (Krishna Swamy *et al.* 1988, hereafter Paper I) has shown that the overall characteristics of the 3–160 μm emission from comet Halley can be matched reasonably well by a model including emission from these two components with silicates dominating the grain material by mass. In this paper, the two-component model described in Paper I is applied to observations of other comets. It is shown that the model can reproduce these observations as well, and that it successfully reproduces pheonomena related to changes in the heliocentric distance of the comets and variations in their grain properties.

While it is known that individual comets can show a great deal of variability on a day-to-day basis, we will argue that most comets produce a general overall pattern of behavior in their infrared emission. It is this pattern in the infrared emission behavior of "normal" comets that is emphasized in this paper.

II. CALCULATION

a) Method

Since a detailed description of the two-component model used in this paper has been presented elsewhere (Paper I), we give only a brief review of the methodology used in our calculations. The 10 and 3.4 μm features in the spectra of comet Halley indicate the presence of at least two dust components, namely, silicates and some form of hydrogenated carbon. These components may exist together in composite particles, or they may reside in separate grains. The model was used to calculate the expected emission from different mixtures of these two components which were assumed to reside in independent particles. An attempt was made to incorporate these materials into the model in a manner which is self-consistent with knowledge derived from studies of collected chondritic IDPs. The chondritic subset of IDPs was used as a guide, since these particles are the most common form of extraterrestrial material found on stratospheric impact collectors (Sandford 1987), and since the elemental abundances of these particles are consistent with those observed by the Halley flyby probes (cf. Brownlee 1988; Jessberger, Christoforidis, and Kissel 1988).

The model uses several approximations for the refractive indices and absorption cross sections of the dust grains. Unfortunately, optical constants are not available for ideal cometary analogs like IDPs. The values we use were taken from

materials which provide the cloest match to the cometary dust we could find from the presently available laboratory data. The silicate component selection was guided by the profiles of the observed 10 μm feature of comet Halley. These profiles can be matched with mixtures of several crystalline silicate minerals common in meteorites and IDPs (Sandford and Walker 1985; Bregman *et al.* 1987). Olivine seems to be the dominant silicate component in comet Halley dust, although lesser amounts of pyroxenes and layer-lattice silicates appear to be present as well. We have used the near- and far-infrared optical properties of the olivine-rich lunar sample 12009.48 for a spectral analog to the silicates in comets (Perry *et al.* 1972). In the ultraviolet and visible regions we use $m = 1.39 - 0.038i$ as these values can explain the observed 0.3–2.25 μm reddening and polarization measurements of several comets (Mukai, Mukai, and Kikuchi 1986; Krishna Swamy and Shah 1988). We note that this refractive index implies that the silicate fraction absorbs more efficiently than a pure, monomineralic sample (Paper I). As with the silicates, there are presently no optical constants available for ideal analogs of cometary carbonaceous materials. We have used the data of Angus, Koidl, and Domitz (1986) for α:C-H films, which consist of partially hydrogenated amorphous carbon. Since relevant data for this material are not available for the ultraviolet and visible spectral regions, the data of Arakawa *et al.* (1985) for evaporated carbon films were used in these spectral regions. Although the optical properties of the silicate and carbonaceous material in comets are certainly not identical with the properties we have assumed, they should provide a reasonable overall approximation. The choice of optical constants is discussed in considerably more detail in Paper I.

Calculation of the grain absorption cross sections were made using Mie theory (van de Hulst 1957). The formalism of Mie theory assumes that the grains are spherical and have homogeneous compositions. In contrast, IDP data and data from the Halley flyby probes suggest that real cometary grains probably have irregular shapes and consist of aggregates of smaller grains having different compositions. Several studies have shown that these complications can produce results not predicted by Mie theory (cf. Hanner 1988 for a recent discussion). In particular, Mie theory often predicts spectral features to be narrower and more highly peaked than seen in the laboratory (cf. Bohren and Huffman 1983). The extent of the applicability of Mie theory depends, of course, on the physical process being considered. In the absence of a theoretical formalism to be used for irregular, heterogeneous particles, we have used the standard Mie theory. The potential limitations of this theory should be kept in mind.

In all the calculations made using Mie theory, we assume that the silicates and amorphous carbon exist as separate particles, i.e., we assume that individual particles *are* homogeneous. Grain temperatures were determined by assuming equilibrium between absorbed solar energy in the ultraviolet and visible spectral regions and emission in the infrared. The size of grains in cometary comae are usually assumed to follow a power-law distribution of the form $n(a) \propto a^{\alpha}$, where a is the radius of the grains and α may have different values over different size ranges (Mazets *et al.* 1986*a*, *b*). For simplicity we will often use a value of $\alpha = -3.5$ for all values of a, since this size distribution produces a reasonable fit to the emission from comet Halley (Paper I) for a realistic grain population composition. Occasionally we will use different power indices valid over different size ranges. In these cases we use α_1 as the index for $a < 6.2$ μm and α_2 for $a > 6.2$ μm (the placement of the transition at $a = 6.2$ μm was chosen to correspond to the endpoint of one of the grain-size regions given in Mazets *et al.* 1986*a*, *b*). These subscript conventions will be used throughout the paper. Our calculations were made assuming minimum and maximum grain sizes of $a = 0.001$ and 100 μm, respectively.

Since it is conceivable that cometary grains may consist of silicate cores with thick carbonaceous mantles, we have also made a number of calculations that assume that all the carbon resides on the silicates. These calculations were made using Güttler's theory (Güttler 1952). The application of Güttler's theory can suffer from the same problems previously mentioned for Mie theory. The limitations discussed for single-composition particles are therefore applicable to the composite grains as well.

Finally, it is necessary to choose the silicate to amorphous carbon mass ratio to be used in the calculations. In Paper I we showed that the thermal emission from comet Halley could be reasonably well fitted by two grain models. If the silicate and amorphous carbon are assumed to reside in independent particles, a good fit to the observational data at all heliocentric distances can be obtained for a silicate to amorphous carbon mass ratio of about 40 to 1. In a similar model in which the grain population is assumed to consist of independent amorphous carbon particles and silicate particles having thin (about 100 Å) "coatings" of amorphous carbon, a similar fit could be obtained, but the silicate to amorphous carbon mass ratio was about 8 to 1. Both cases require compositions that are reasonably consistent with those observed in IDPs. In contrast, a model in which all the carbon is assumed to reside in thick mantles surrounding the silicates (core-mantle grains) provides a worse spectral fit and requires silicate to amorphous carbon mass ratios of unity or greater. This is considerably more carbon than is seen in IDPs and has the additional disadvantage that it assumes a particle morphology that is rarely seen in IDPs. For simplicity, the calculations made in this paper for comparison with cometary data were done assuming that the grain populations consist of independent silicate and amorphous carbon particles in a mass ratio of 40 to 1. We note that the silicate to carbon mass ratio observed in IDPs may represent an upper limit for cometary grains, as the collected grains may have lost a carbonaceous component of intermediate volatility between cometary ejection and collection in the stratosphere. If the appropriate silicate to amorphous carbon mass ratio is, in fact, less than 40 to 1, the model which assumes that all the silicates have thin coatings of carbonaceous material provides a better compositional match to the data. The general spectral behaviors of the coated and uncoated silicate models are qualitatively similar. Consequently, the conclusions we will reach are valid for silicate to amorphous carbon ratios spanning the range of reasonable values.

b) Results

Before proceeding with a detailed comparison between the two-component model and the observations, it is informative to examine the dependence of the model on the various parameters in the calculations. Figures 2, 3, and 4 present model calculations in which the parameters associated with heliocentric distance, the mass fraction of silicates relative to carbonaceous material, particle size, and particle morphology are varied. The results demonstrate several important points associated with the 10 μm feature.

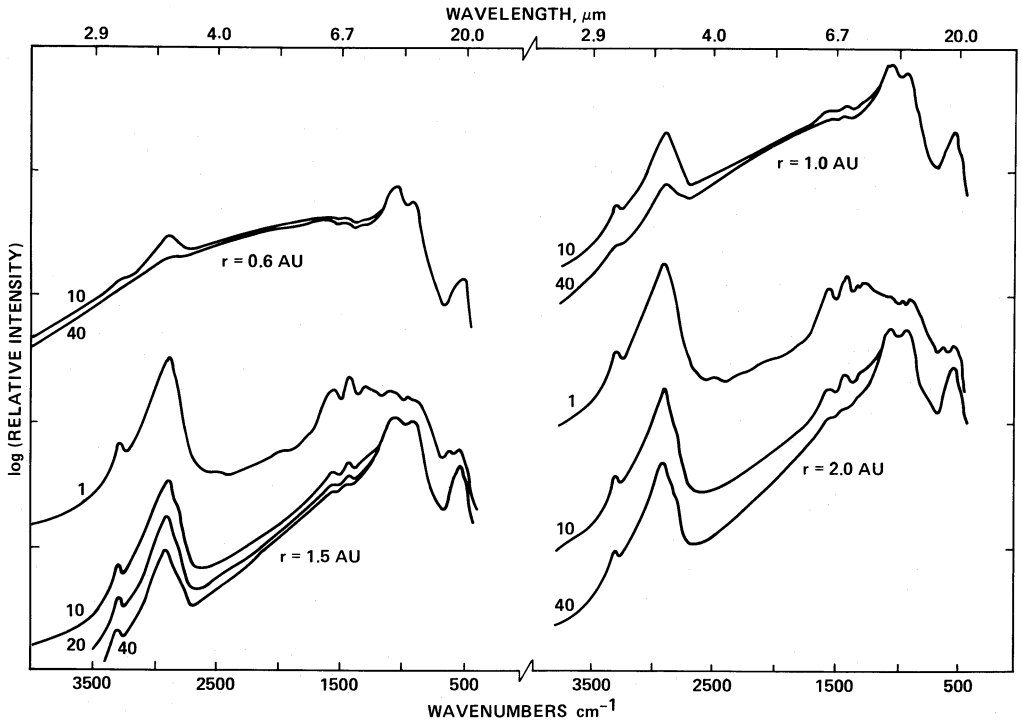

FIG. 2.—Emission produced by a mixture of silicate and amorphous carbon particles having a grain-size distribution defined by the power-law index $\alpha = -3.5$. Grain temperatures were calculated assuming thermal equilibrium at heliocentric distances of 0.6, 1.0, 1.5, and 2.0 AU. The assumed mass ratio of silicate to amorphous carbon grains is shown for each curve.

Figure 2 presents the calculated emission from cometary grains at several heliocentric distances ($r = 0.6$, 1.0, 1.5, and 2.0 AU). The calculations have been made using different silicate to amorphous carbon mass ratios for each distance. The figure demonstrates that, at any given heliocentric distance, the contrast of the 10 μm feature to the continuum decreases as the contribution from amorphous carbon particles increases. The 10 μm feature disappears entirely if comparable amounts of carbonaceous material and silicates are present. In this case, however, several new spectral features due to C-C vibrational modes appear in the 6–7 μm region.

It is often assumed that the absence of an obvious 10 μm band in the spectrum of a comet implied that either (1) no silicates were present or (2) the silicates were masked by carbonaceous material. Figure 2 shows that the latter possibility is unlikely, since the 10 μm band is not masked until the silicate to amorphous carbon mass ratio drops to values as low as unity. At these concentrations the carbonaceous material should be producing C-C bands in the 6–7 μm region, bands which have not been seen in cometary data (although, in all fairness, we must point out that appropriate observations are few in number). Furthermore, silicate to amorphous carbon mass ratios as low as unity lie *far* below the values of 10–50 typical of IDPs (Bradley, Brownlee, and Fraundorf 1984), many of which are thought to be derived from comets (Sandford 1987). In the past, the observed low albedos of comets (see Hanner 1986 for a review) have been attributed to carbonaceous materials and used as an argument in favor of their predominance in comets. The low albedo of a dust grain does not, however, necessarily imply that the grain is made up predominantly of dark material. This point is amply demonstrated by collected IDPs. These grains are dominated by silicates (Sandford and Walker 1985) and contain only 2%–10% carbonaceous material by mass (Bradley, Brownlee, and Fraundorf 1984). Much of the carbonaceous material resides in a "matrix" phase in which the silicate minerals are embedded. Since the carbonaceous material is relatively opaque to visible light, it is this component which dominates the optical properties of the particle in the visible spectral region (Allamandola, Sandford, and Wopenka 1987; Paper I), despite its lower abundance.

Thus, the lack of strong features in the 5–8 μm region in Halley spectra, the presence of 10 μm features in many cometary spectra, and the elemental abundances and morphologies observed in IDPs lead us to conclude that silicates dominate the mass distribution of the emitting refractories in comets. As discussed earlier, unless stated otherwise, all our calculations have been made assuming a silicate to amorphous carbon mass ratio of 40 to 1.

The effect of grain-size distribution is examined in Figure 3. A mass ratio of silicate to amorphous carbon of 40 was assumed in all cases. Calculations were made for the same solar distances given in Figure 2, but using different indices for the size distribution ($\alpha = -2.0$, -3.0, and -3.5). As can be seen, the contrast of the 10 μm feature with its adjacent continuum depends upon the grain-size distribution of the silicate particles. As the larger grains become more important, the feature becomes weaker and finally disappears (Krishna Swamy and Donn 1979; Paper I). Clearly the absence of an obvious 10 μm feature in the spectrum of a comet *does not* necessarily imply that no silicates are present. Instead, large grains may be dominating the emission. This effect has been noted earlier by Ney (1974*a*) and others.

Since we have previously shown (Paper I) that core-mantle grains cannot simultaneously provide a good spectral match to comet Halley data and a good compositional match to the

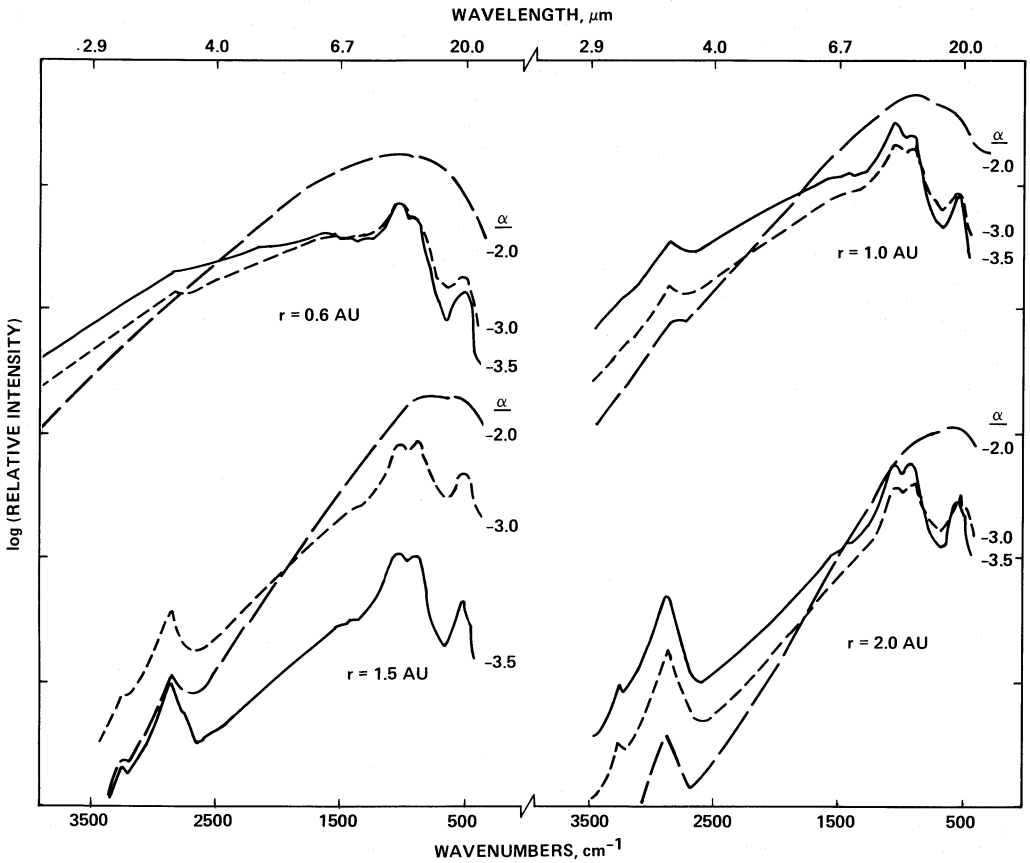

FIG. 3.—Emission, as a function of α, produced by a mixture of silicate and amorphous carbon particles having a mass ratio of 40 to 1 at heliocentric distances of 0.6, 1.0, 1.5, and 2.0 AU.

IDPs, we will not discuss this type of particle in any detail here. Figure 4 shows an example of the results of calculations using Güttler's theory for grains having silicate cores with $a = 0.1$ μm and mantles of amorphous carbon of various thicknesses. Grain temperatures of 300 and 400 K were used. The results are quite similar to those shown in Figure 2, where the fraction of independent amorphous carbon grains was varied. Again, we see that the 10 μm silicate feature can be masked if sufficient carbon is present. There are several reasons, however, why it is unlikely that thickly mantled grains are responsible for cometary emission spectra that show no obvious 10 μm feature. Some of the objections are the same as those listed in conjunction with Figure 2, namely, the addition of mantles thick enough to mask the silicate feature results in (1) composite grains with silicate to amorphous carbon mass ratios much lower than those seen in IDPs and (2) spectra with strong emission features in the 6–7 μm region. An additional objection is provided by the observation that core-mantle grains of this type are very rare in IDPs.

III. COMPARISON BETWEEN THE MODEL AND OBSERVATIONS

a) Comparisons with Cometary Data

In Paper I it was shown that the two-component model in which the silicates and amorphous carbon reside in independent particles produces calculated emission curves which fit reasonably well with a variety of moderate-resolution infrared observations of comet Halley from about 3 to 160 μm. The best fits required mass ratios of silicate to amorphous carbon between 40 to 1 and 8 to 1, depending on whether the silicates were assumed to consist of bare particles or have thin (< 100 Å) coatings of carbonaceous material. Both calculations reproduce the profile of the 10 μm feature observed at medium resolution quite well. In general it was found that the amorphous carbon dominates the emission in the wavelength region around 3–4 μm, while the silicates dominate at wavelengths above 4 μm.

In view of the success of the two-component model in fitting the moderate-resolution data from Halley, it is interesting to test its applicability to other infrared observations as well. These include both broad-band observations of comet Halley and observations of other comets. Table 1 provides a summary of the cometary data we will examine in the following discussion. Each entry includes the name of the comet, the spectral range of the observations, the observation date, the comet's heliocentric distance, and the reference from which the cometary data are taken.

A comparison between the two-component model predictions and broad-band observations of comet Halley is shown in Figure 5. Comet Halley was monitored using broad-band photometry by a variety of observers at regular intervals starting at a heliocentric distance of about 28 AU and continuing beyond perihelion passage. The model calculations were made assuming that the mass ratio of silicate particles to amorphous carbon particles was 40 and that the two components reside in independent particles. The range in size distributions which best fit the data include $\alpha_1 = -3.5$ and $\alpha_2 = -3.2$ (*solid lines*) and $\alpha_1 = -3.5$ and $\alpha_2 = -3.0$ or -2.5 (*dashed lines*). At large heliocentric distances there are only two observational data points available centered at about 10.1 and 20.0 μm (see Fig.

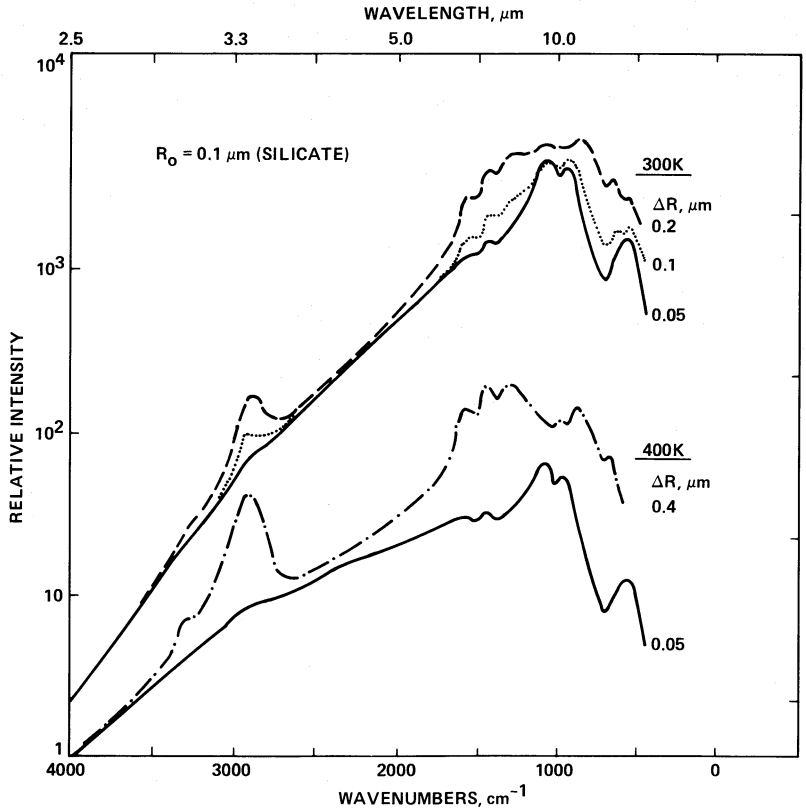

FIG. 4.—Calculated emission from composite grains consisting of silicate cores surrounded by amorphous carbon mantles. Calculations were made assuming grain temperatures of 300 and 400 K. Core radii were assumed to be 0.1 μm, and the mantle thickness (ΔR) was varied. The mantle thickness is listed for each curve.

TABLE 1

SUMMARY OF OBSERVATIONS USED IN THIS PAPER

Comet	Wavelength Region (μm)	Date	Heliocentric Distance (AU)	Reference
Churyumov-Gerasimenko	1.25–20.0	1982 Nov 16	1.35	1
Grigg-Skjellerup	1.25–20.0	1982 Jun 23–28	1.15	2
Halley	1.25–19.2	1985 Aug 24–1986 Mar 31	1.2–2.8	3
	1.25–20.0	1985 Aug 25–1986 Jan 8	0.9–2.8	4
	2.8–3.7	1986 May 19, 20	1.9	5
	5.0–10.0	1985 Dec 12	1.32	6
	8.0–13.0	1985 Dec 17	1.32	6
	5.0–10.0	1986 Apr 8	1.32	6
	2.8–3.8	1986 Mar 26–Apr 25	1.1–1.59	7
	8.2–12.8	1986 Jan 26	0.67	8
	0.7–18.0	1986 Feb 12	0.59	9
	2.2–18.0	1986 Mar 28	1.12	9
IRAS-Araki-Alcock	8.0–13.0	1983 May 11	1.0	10
	2.0–4.0	1983 May 12	1.0	10
Kohoutek	0.55–18.0	1974 Jan 1	0.23	11
Stephan-Oterma	4.8–20.0	1980 Nov 26	1.58	2
West	0.55–18.0	1976 Feb 2–1976 Apr 5	0.2–1.0	12

REFERENCES.—(1) Hanner *et al.* 1985*b*; (2) Hanner *et al.* 1984; (3) Green *et al.* 1986; (4) Tokunaga *et al.* 1986; (5) Tokunaga, Nagata, and Smith 1987; (6) Bregman *et al.* 1987; (7) Knacke, Brooke, and Joyce 1986; (8) Bouchet *et al.* 1987; (9) Gehrz and Ney 1986; (10) Hanner *et al.* 1985*a*; (11) Ney 1974*b*; (12) Ney and Merrill 1976.

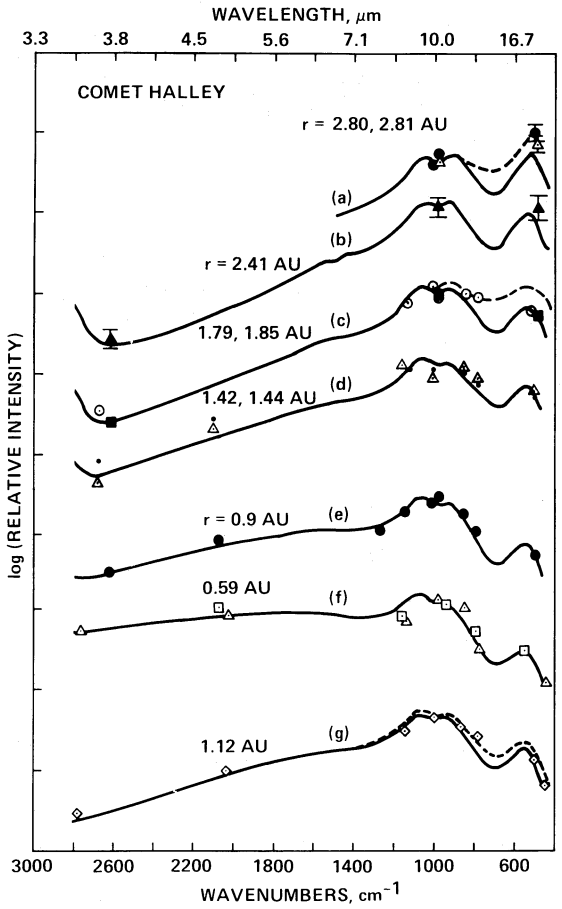

FIG. 5.—Comparison of the calculated and observed infrared emission from comet Halley at various heliocentric distances. (*a*) $r = 2.80$ AU (Green *et al.* 1986); *open triangles*: $r = 2.81$ AU (Tokunaga *et al.* 1986). (*b*) *Filled triangles*: $r = 2.41$ AU (Tokunaga *et al.* 1986). (*c*) *Filled squares*: $r = 1.85$ AU (Tokunaga *et al.* 1986); *open circles*: $r = 1.79$ AU (Green *et al.* 1986). (*d*) *Open triangles*: $r = 1.44$ AU (Green *et al.* 1986); *solid dots*: $r = 1.42$ AU (Green *et al.* 1986). (*e*) *Filled circles*: $r = 0.9$ AU (Tokunaga *et al.* 1986). (*f*) *Open triangles*: $r = 0.59$ AU, 1986 February 9 (Gehrz and Ney 1986); *open squares*: $r = 0.59$ AU, 1986 February 12 (Gehrz and Ney 1986). (*g*) *Open diamonds*:) $r = 1.12$ AU (Gehrz and Ney 1986). Calculated curves (assuming a silicate to amorphous carbon ratio of 40): (*a–g*) *solid curve*: $\alpha_1 = -3.5$, $\alpha_2 = -3.2$; (*a*, *c*) *dashed curve*: $\alpha_1 = -3.5, \alpha_2 = -2.5$; (*g*) *dashed curve*: $\alpha_1 = -3.5, \alpha_2 = -3.0$.

5*a*). The vertical positions of the model curves shown for $r = 2.4$ and 2.8 AU are based on the assumption that these two observational points correspond to the 10 and 20 μm features predicted by the theory. The agreement between the model profile and the observations is good over the entire range of heliocentric distances and wavelengths. The model produces the correct slope of the continuum between 4 and 10 μm and also reproduces the relative flux between 10 and 20 μm reasonably well.

We note that comparisons of the observed and modeled relative strengths of the 10 and 20 μm silicate features are subject to several uncertainties. First, as can be seen in Figure 5, the apparent relative strength of the two features is sensitive to the number of larger grains in the grain-size distribution. An increase in the number of larger dust grains produces additional thermal flux at longer wavelengths and results in an apparent relative enhancement of the 20 μm feature (see, for example, Figs. 5*a*, 5*c*, and 5*g*). An additional complication arises from the nature of the 20 μm data. Many of these data are taken using filters with very large bandpasses (up to 8 μm) and thus represent only an average flux in the 20 μm region. Thus, the match between the data and the model demonstrates general consistency, but the uncertainties preclude detailed comparison of the model with the 20 μm data.

A similar comparison with the broad-band infrared observations of comet West is shown in Figure 6. The solid lines represent the model results assuming independent silicate and amorphous carbon particles having a mass ratio of 40, $\alpha_1 = -3.5$, and $\alpha_2 = -3.2$. Again, the agreement between the observations and calculations is very good over the entire wavelength region at all heliocentric distances.

At this point it is appropriate to make a few remarks regarding the values of α_1 and α_2 used in the model calculations. The values of $\alpha_1 = -3.5$ and $\alpha_2 = -3.2$ provide a better fit to the data than a simple $\alpha = -3.5$ power law, i.e., slightly larger grains are probably responsible. In principle it is not unreasonable to expect the grain-size distribution in cometary comae to change with time. Such changes could occur both in a regular fashion (due to temperature-dependent, i.e., heliocentric, effects) and sporadically (due to outbursts and related phenomena). Since the broad-band points near 12 μm are not significantly higher than the solid curves and since they contain poorly defined contributions from both the 10 μm silicate band and its adjacent continuum, it is not clear at the present time whether our calculational refinement represents a real change in the nature of the dust.

There are examples that demonstrate that differences in grain-size distributions *can* be important. Figure 7 shows the comparison between our model calculations and broad-band infrared measurements of comet Kohoutek when it was at a heliocentric distance of $r = 0.23$ AU. Observations were made of the tail, the antitail, and the coma (Ney 1974*a*, *b*). The presence of a 10 μm feature is apparent in the spectra of the tail and coma, but it is not as obvious in the antitail. The shape of the observed continuum between 3 and 8 μm is similar for all three spectra and is similar to that of comet West at a comparable heliocentric distance. This implies that $\alpha_1 = -3.5$ is appropriate for all three observations. The lack of an obvious 10 μm feature in the spectrum of the antitail suggests that grains which are "larger than normal" may be present, as already noted by Ney (1974*a*). Indeed, the calculated curves provide a better fit to the data if it is assumed that $\alpha_2 = -2.5$ for dust in the antitail and $\alpha_2 = -3.0$ for dust in the tail and coma. While the lack of an obvious 10 μm feature in the antitail could be due to differences in the composition of the dust grains in the antitail, it is more likely that the differences are due to size effects. This interpretation is especially preferable because there are good reasons related to orbital dynamics for expecting larger grains to be present in the antitail (Ney 1974*a*, *b*; Krishna Swamy and Donn 1979; Gary and O'Dell 1974).

Comet IRAS-Araki-Alcock provides another example of a comet that shows evidence for "larger than normal" grains. Moderate-resolution data taken when the comet was at $r = 1.0$ AU do not show an obvious 10 μm feature (Hanner *et al.* 1985*a*). As can be seen in Figures 8*a* and 8*b*, the standard values of $\alpha_1 = -3.5$ and $\alpha_2 = -3.2$ do not provide a very good fit to the data. In Figure 8*b* we compare the spectrum of the coma around the nucleus of the comet with several calculations made assuming that larger grains are present. Larger grains do provide a better fit, although it is difficult to discriminate between the various possibilities using the 10 μm data

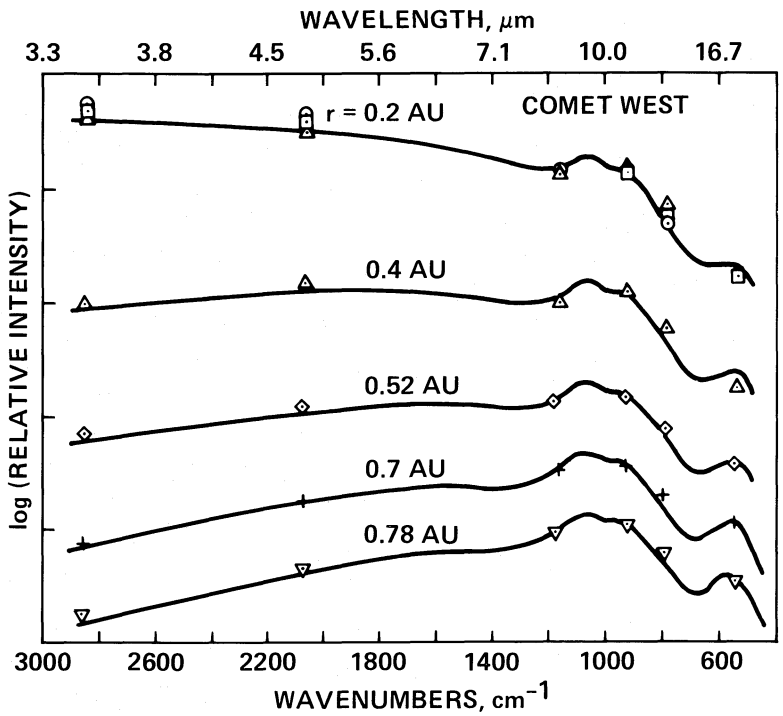

FIG. 6.—Comparison of the calculated and observed 3.4–25 μm emission from comet West at solar distances of 0.2, 0.4, 0.52, 0.7, and 0.78 AU (observations from Ney and Merrill 1976). Model curves were made assuming $\alpha_1 = -3.5$, $\alpha_2 = -3.2$, and a silicate to amorphous carbon mass ratio of 40.

alone. The additional short-wavelength data of Hanner *et al.* (1985*a*) demonstrate that the $\alpha_1 = -3.5$ and $\alpha_2 = -2.0$ model provides the best fit. A similar comparison is shown in Figure 8c where the observational data were taken of the coma 16″ north of the nucleus. This spectrum is representative of a number of positions measured around the nucleus. The best fit is again provided by the $\alpha_1 = -3.5$ and $\alpha_2 = -2.0$ calculation. Thus, in the spectra in which we require an increased contribution from larger grains, the inflection in the grain-size distribution bends in the sense opposite to that inferred for comet Halley (Mazets *et al.* 1986*a*, *b*).

The lack of an obvious silicate feature could presumably also be due to an increased amorphous carbon to silicate ratio (see Fig. 2). However, model calculations with larger contributions from carbonaceous material fail to provide the correct slope in the 4–8 μm region needed to link the long- and short-wavelength data. The differences between the model and the data in the 3.4 μm region (Fig. 8*b*) also suggest a problem with

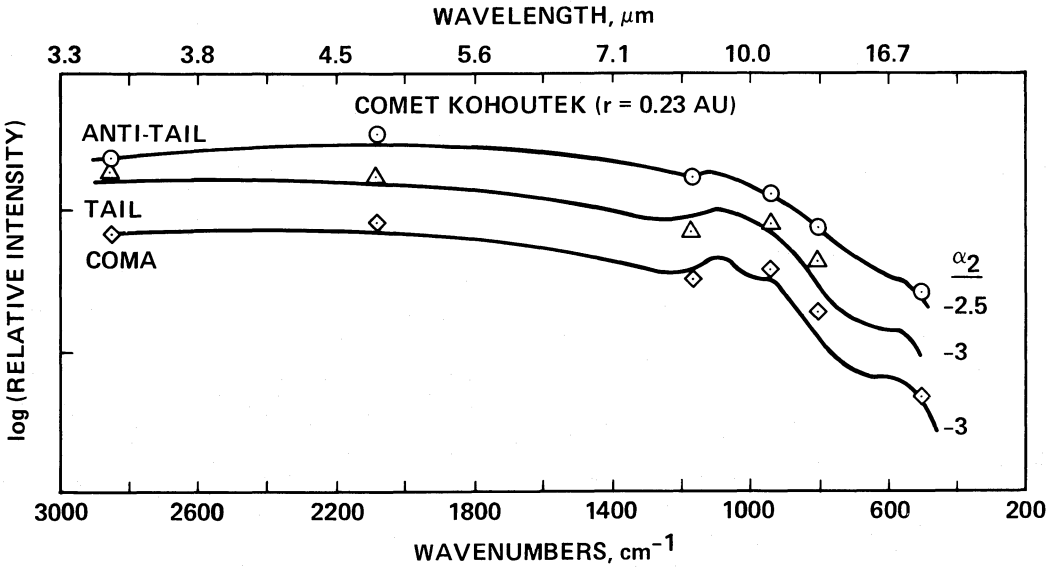

FIG. 7.—Comparison of the calculated and observed infrared emission from comet Kohoutek at $r = 0.23$ AU. The observations are from Ney (1974*b*). The continous curves are the calculated results assuming a silicate to amorphous carbon mass ratio of 40, $\alpha_1 = -3.5$, and the various listed values for α_2.

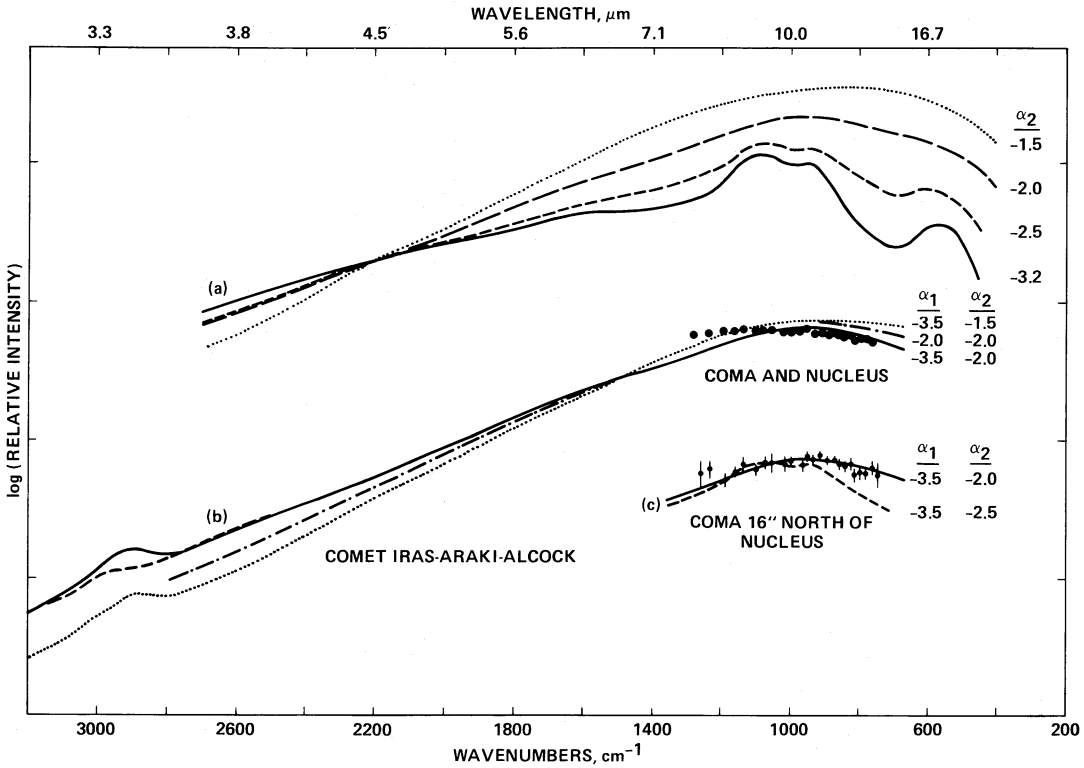

FIG. 8.—Comparison of the calculated and observed infrared emission from comet IRAS-Araki-Alcock. (*a*) Calculated emission curves assuming different values of α_2, and $\alpha_1 = -3.5$. The curves have been arbitrarily normalized at 2200 cm^{-1} (4.5 μm). All the model curves in this figure were made assuming a silicate to amorphous carbon ratio of 40. (*b*) Observations: solid dots near 10 μm and dashed line near 3.4 μm, $r = 1.0$ AU, coma surrounding the nucleus of the comet (Hanner *et al.* 1985*a*). Calculated curves: *continuous*: $\alpha_1 = -3.5$, $\alpha_2 = -2.0$; *dotted*: $\alpha_1 = -3.5$, $\alpha_2 = -1.5$; *dot-dash*: $\alpha_1 = \alpha_2 = -2.0$. (*c*) *Solid dots*: $r = 1.0$ AU, coma 16″ north of the nucleus (Hanner *et al.* 1985*a*). Calculated curves; *continuous*: $\alpha_1 = -3.5, \alpha_2 = -2.0$; *dashed*: $\alpha_1 = -3.5, \alpha_2 = -2.5$.

this interpretation. The model, which assumes that the carbonaceous material constitutes *only 1 part in 40* (i.e., a value typical of IDPs and primitive meteorites), predicts a small but distinct emission feature at 3.45 μm. While there may be a hint of such a band in the cometary data, it is clearly considerably weaker than the model predicts. This is inconsistent with the interpretation that comets are dominated by carbonaceous materials unless the material is extremely hydrogen-poor. However, much of the carbonaceous material in IDPs is known to consist of hydrocarbons (McKeegan, Walker, and Zinner 1985), and graphite, a hydrogen-poor carbonaceous material, is *not* a common component in IDPs. These, and the additional arguments stated in § II*b*, suggest that an increased relative abundance of carbonaceous material is not likely to be responsible for the lack of a silicate feature. We are led to conclude that the mean size of the particles in all the measured positions around comet IRAS-Araki-Alcock is probably much larger than in normal (i.e., Halley-like) comets.

Finally, as an aside, we note that the observed 3.4 μm feature in the spectrum of IRAS-Araki-Alcock, if it is real, falls at slightly shorter wavelengths than are predicted by our model. This result is similar to that noted in Paper I for comet Halley. We will return to this point later.

In summary, consideration of the model comparisons with comets Kohoutek and IRAS-Araki-Alcock shows that it is possible (in fact, probable) that silicates are the dominant refractory component in cometary grain mixtures *even when no 10 μm feature is evident in the spectra.*

b) Calculation of Grain Temperatures

It is apparent from the previous comparisons that the broad-band data, while often capable of determining whether or not a 10 μm band is present in a cometary spectrum, does a poor job of defining the absolute strength of the feature. Data points falling near the peaks of the 10 and 20 μm features provide little information about the strengths of these bands when unaccompanied by observations of the adjacent continuum. This often makes it difficult to define uniquely the underlying continuum levels. Since the continuum contribution to the broad-band data is used to determine the temperature of the observed dust, it is appropriate to discuss the effects this ambiguity has on the determination of grain temperatures.

The dust temperature is generally estimated from the spectra by comparing the profile of the observed points with various blackbody curves. In general, if the real part of the index of refraction (n) is near unity, then for $x = 2\pi a/\lambda < 1$, the absorption efficiency of the grain is given by $Q_{abs} \simeq 8xk/3$, where k is the complex part of the refractive index $m = n - ik$. In these limits the emission, given by $B(\lambda, T_g)Q_{abs}$, scales as $B(\lambda, T_g)$, i.e., as a blackbody. Of course, there actually is no "unique" temperature associated with the dust in a cometary coma. Stated temperatures of the dust represent approximations to an average, since the true temperatures of individual grains vary depending on their size and composition. This point should always be kept in mind.

Unfortunately, the presence *or apparent absence* of a 10 μm

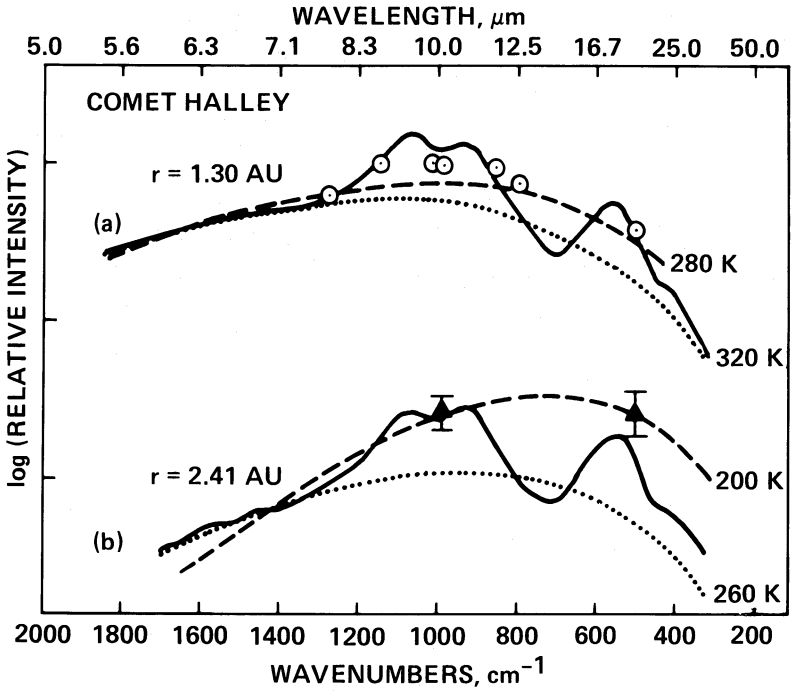

FIG. 9.—Comparison of the calculated and observed emission from comet Halley at $r = 1.30$ and 2.41 AU (observational data from Tokunaga *et al.* 1986). Model curves assumed a silicate to amorphous carbon mass ratio of 40, $\alpha_1 = -3.5$, and $\alpha_2 = -3.2$. The dashed and dotted curves are the blackbody fits to the observations and the model curves, respectively.

feature in the observations can have an effect on the grain "temperature" deduced from the data. Several examples of this are provided by the comet Halley data shown in Figure 9. The data points in Figure 9*a* correspond to a heliocentric distance of $r = 1.30$ AU and can be fitted by a blackbody curve corresponding to a temperature of about 280 K (*dashed curve*) if one assumes that no silicate features are present (Tokunaga *et al.* 1986). Superposed on the data is a solid curve corresponding to the emission predicted by our two-component model. As can be seen, the model spectrum clearly shows the presence of silicate features. The best fit to the continuum under the theoretical curve is provided by a 320 K blackbody (*dotted curve*). This is substantially higher than the temperature that is predicted without the model. The higher temperature is probably more representative of the correct "mean" of the temperature distribution, since the 5–8 μm moderate-resolution continuum data taken by Bregman *et al.* (1987) at about the same heliocentric distance are best fitted by a 320 K blackbody curve.

Another example of how the 10 and 20 μm data points can be misleading is shown in Figure 9*b*. The 10 and 20 μm data points were taken when Halley was at $r = 2.41$ AU. The points are compared with blackbody curves assuming either (1) that the points correspond to the continuum (*dashed curve*) or (2) that they correspond to the peaks of the 10 and 20 μm features predicted by our model (*solid curve*). Again, a direct blackbody fit to the two data points gives a lower mean temperature than that derived by fitting only the continuum.

It is clearly misleading to fit blackbody curves to data in the 10 and 20 μm regions. In general the profile of the 10 μm feature starts near 8 μm and the continuum is reasonably well defined in the 4–8 μm region. In estimating the blackbody temperature, one should avoid the 10 μm feature and fit to other data points. Since the 5–8 μm region in Halley was largely devoid of emission bands (Bregman *et al.* 1987), it provides the best region for mean temperature determinations.

Figure 10 shows several plots of the variation of blackbody grain temperatures as a function of heliocentric distance. The dashed line is a fit to derived average grain temperatures found in the literature, while the solid line is a fit to the temperatures we infer from the same cometary data using our model. The model calculations were made assuming that the emission was produced by independent silicate and amorphous carbon particles having a relative mass ratio of 40 to 1. Only those comets which could be fitted by an $\alpha_1 = -3.5$ and $\alpha_2 = -3.2$ size distribution are shown in the figure. For comparison, the dotted line represents the expected temperature behavior if the dust behaves like a perfect blackbody. The relation $T = 375r^{-0.43}$ fits the model grain temperature points (*solid line*). This can be compared with a relation $T = 329r^{-0.53}$ (*dashed line*) for the literature data (Eaton 1984). Figure 10 demonstrates that models which assume that cometary materials behave as perfect blackbodies are likely to underestimate the grain temperatures substantially. For example, at a heliocentric distance of $r = 1.0$ AU the predicted blackbody temperature is about 300 K, while the mean of the temperature distribution is probably nearer to 400 K. Thus, cometary models based simply on blackbody temperatures are likely to predict inappropriate heliocentric behavior for processes involving sublimation and other temperature-dependent properties.

c) *The* C-H *Stretch Feature*

One of the more important discoveries made during the recent apparition of comet Halley was the detection of an emission feature near 3.4 μm (Wickramasinghe and Allen 1986; Knacke, Brooke, and Joyce 1986; Danks *et al.* 1987; Baas,

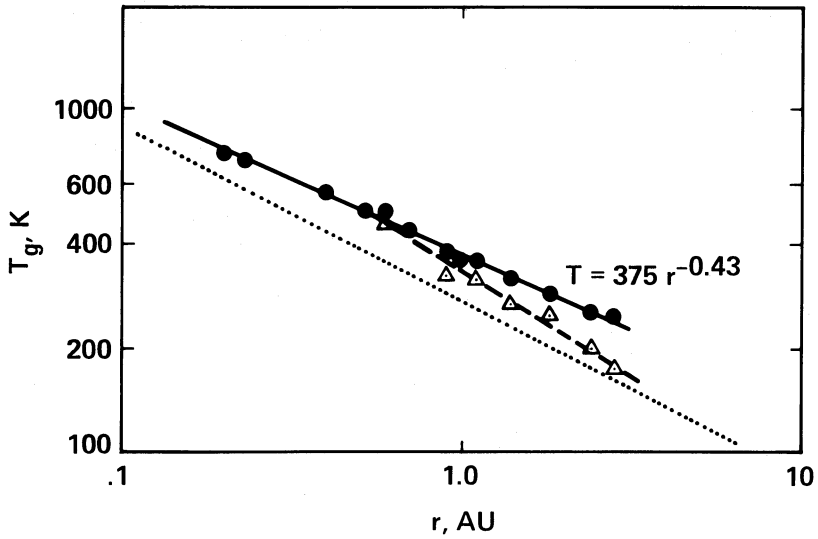

FIG. 10.—Derived mean grain temperatures as a function of cometary heliocentric distance. *Filled circles*: temperatures determined from individual spectra using the model fit to the points; *open triangles*: temperatures determined directly from broad-band Halley data (Tokunaga *et al.* 1986; Green *et al.* 1986; Gehrz and Ney 1986; Bregman *et al.* 1987). The solid curve is fitted to the model temperature determinations and can be functionally described by $T = 375r^{-0.43}$. This can be compared with the expression $T = 329r^{-0.53}$ derived by Eaton (1984) from the literature data (*dashed curve*). The dotted curve represents the temperature behavior of a perfect blackbody and is provided for reference.

Geballe, and Walther 1986; Tokunaga, Nagata, and Smith 1987). These observations clearly show a feature whose strength varies with heliocentric distance. Depending upon the heliocentric distance of the comet, the feature lies on a background continuum dominated by thermal emission from the cometary dust, scattered incident solar radiation, or a combination of the two. The 3.4 μm feature is generally attributed to C-H stretching vibrations. Two physical emission mechanisms have been suggested to explain the feature. First, the feature could be due to a fluorescence process where high-energy photons excite large molecules in the coma which subsequently relax by fluorescing (Baas, Geballe, and Walther 1986). Second, the band could arise from simple thermal emission from carbonaceous grains.

It has been shown in Paper I and by others (Wickramasinghe *et al.* 1986; Chyba and Sagan 1987) that thermal emission from amorphous carbon grains or carbonaceous residues could, in principle, account for the 3.4 μm feature in comet Halley. In the discussion that follows, we compare observations of the 3.4 μm feature with our thermal emission model. Recall that the variation of the strength of the 3.4 μm feature as a function of the silicate to amorphous carbon mass ratio, heliocentric distance (i.e., grain temperature), and grain size can be found in Figures 2 and 3 and in Paper I.

Figure 11 shows broad-band measurements between 1.25 and 20 μm taken from comet Halley when it was at heliocentric distances of about 0.6, 0.9, 1.4, 1.8, and 2.4 AU. The solid curves plotted for $\lambda \geq 3.2$ μm are the calculated emission assuming a mass ratio of silicate to amorphous carbon of 40 and a grain-size distribution given by $\alpha_1 = -3.5$ and $\alpha_2 = -3.2$. The dashed lines plotted between 1.25 and 3.2 μm represent the added contribution of scattered solar radiation as defined by the short-wavelength broad-band points (the shape of the curve for $\lambda \leq 2.2$ μm in the $r = 0.6$ AU case is assumed to have the same shape as those of the other curves, since measurements are not available). In several cases these data were taken at heliocentric distances corresponding roughly to the distances at which higher resolution measurements of the 3.4 μm feature were made. The higher resolution data are represented by the dotted lines in the middle three spectra. It is apparent from Figure 11 that the continuum on which the 3.4 μm feature falls is dominated by thermal emission from the coma at small heliocentric distances. As the heliocentric distance increases, the thermal continuum falls and the continuum at 3.4 μm gradually becomes dominated by scattered solar radiation. In the case of comet Halley, this transition occurs somewhere between 0.9 and 1.4 AU.

The moderate-resolution spectra of the 3.4 μm feature shown in the figure demonstrate that the spectral "contrast" of the band increases as the comet moves away from the Sun. This aspect of the feature has a simple explanation and is adequately reproduced by the model calculations. At small heliocentric distances the silicate grains are quite hot, and following the blackbody emissivity law, they emit a substantial amount of radiation at shorter wavelengths. This radiation raises the continuum level near the feature and overwhelms the 3.4 μm band and the scattered solar continuum. At larger heliocentric distances the silicates are cooler, they emit less short-wavelength radiation, and they produce a lower thermal continuum in the vicinity of the 3.4 μm feature. Thus, the thermal emission approach qualitatively reproduces the behavior of the 3.4 μm feature. This should not be taken as definitive evidence that fluorescence processes are not occurring, however, since they may produce similar behavior. Future work will be necessary before the thermal emission versus fluorescence issue can be resolved.

As noted earlier in the discussion of Figure 8, the band position derived from the model peaks at a slightly longer wavelength than is seen in the cometary data. This mismatch is especially obvious in Figure 11. As with any spectral feature produced by molecular vibrations, the exact location of the 3.4 μm feature depends upon the molecular structure to which the C-H group is attached. The mismatch in band positions in Figure 11 demonstrates that the α:C-H films from which our optical constants are taken do not provide a perfect analog to

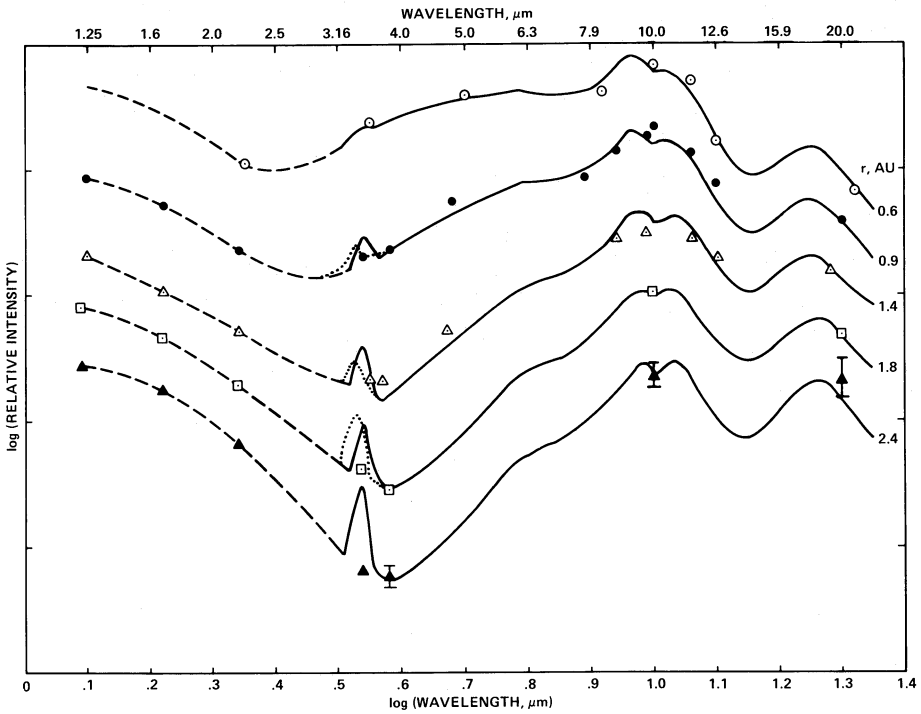

FIG. 11.—Comparison of the calculated and observed 1.25–20 μm spectra of comet Halley as a function of heliocentric distance. The continuous curves were calculated assuming a silicate to amorphous carbon mass ratio of 40, $\alpha_1 = -3.5$, and $\alpha_2 = -3.2$. The dashed curves are hand-drawn fits to the observed scattered solar continuum. The observed profile of the 3.4 μm feature is represented by dotted lines in the middle three spectra. The 3.4 μm data are from Knacke, Brooke, and Joyce (1986) and Tokunaga, Nagata, and Smith (1987). The broad-band data are shown as symbols. *Open circles*: $r = 0.6$ AU (Gehrz and Ney 1986); *filled circles*: $r = 0.9$ AU (Tokunaga *et al.* 1986); *open triangles*: $r = 1.4$ AU (Green *et al.* 1986); *open squares*: $r = 1.8$ AU (Green *et al.* 1986); *filled triangles*: $r = 2.4$ AU (Tokunaga *et al.* 1986).

the molecular subgroups present in the carbonaceous material in comet Halley. It is important to note that the C-H stretch feature found in the spectrum of comet Wilson (Allen and Wickramasinghe 1987), and the tentative C-H stretch feature in the spectrum of comet IRAS-Araki-Alcock (Fig. 8), also fall at shorter wavelengths than the feature produced by α:C-H films. The shorter wavelength of the cometary feature suggests that the material in comet Halley may be richer in aromatic molecular structures than the α:C-H films we have used.

While the band position and strength are sensitive to the molecular structure of the carbonaceous material, the continuum is relatively insensitive to such effects. Thus, while the α:C-H films do not provide a perfect analog to the material in comet Halley, they do provide a reasonable indication of the general effect carbonaceous materials have on the emission spectra of comets. These points are discussed in more detail in Paper I.

IV. CONCLUSIONS

The observed heliocentric variation of 3–20 μm infrared emission from cometary dust can be reproduced quite well using a two-component model based on a mixture of independent silicate and amorphous carbon particles having a mass ratio in the 40-to-1 to 8-to-1 range with a grain-size distribution defined by a power index of $\alpha \simeq -3.5$. The 40:1 mass ratio corresponds to the presence of "bare" silicates, whereas the 8:1 ratio corresponds to the presence of silicates having thin (< 100 Å) "coatings." Reasonable spectral fits can also be found using other silicate to carbon mass ratios and particle size distributions. However, the parameters we have used here have the advantage that, in addition to providing good spectral matches, they are consistent with elemental and morphological constaints provided by collected interplanetary dust particles (IDPs) and Halley flyby data. Silicate minerals can be the dominant component producing emission at wavelengths longward of 4 μm, even in comets which produce no obvious 10 μm silicate feature. The most likely explanation of cometary spectra lacking a 10 μm feature is the presence of larger silicate grains rather than increased amounts of carbonaceous materials.

The model produces a good match to data taken from the same comet at different heliocentric distances. This demonstrates that the variation of grain temperature with heliocentric distance accounts for the major changes observed in cometary spectra.

Blackbody fits to broad-band infrared data can yield unrealistically low grain temperatures if the contributions of the 10 and 20 μm silicate emission bands are not properly taken into account. It is generally better to determine the grain temperature distribution using 4–8 μm data, since this spectral region is devoid of major emission features.

Finally, the model qualitatively reproduces the heliocentric variation of the strength of the 3.4 μm feature seen in comet Halley spectra but does not match it in spectral position or profile.

The authors would like to thank an anonymous referee whose careful reading and helpful comments have resulted in an improved version of this paper.

REFERENCES

Allamandola, L. J., Sandford, S. A., and Wopenka, B. 1987, *Science*, **237**, 56.
Allen, D. A., and Wickramasinghe, D. T. 1987, *Nature*, **329**, 615.
Angus, J. C., Koidl, P., and Domitz, S. 1986, in *Plasma Deposited Thin Films*, ed. J. Mort and F. Jansen (Boca Raton: CRC Press), p. 89.
Arakawa, T., Dolfini, S. M., Ashley, J. C., and Williams, M. W. 1985, *Phys. Rev. B*, **31**, 8097.
Baas, F., Geballe, T. R., and Walther, D. M. 1986, *Ap. J.* (*Letters*), **311**, L97.
Becklin, E. E., and Westphal, J. A. 1966, *Ap. J.*, **145**, 445.
Bohren, C. F., and Huffman, D. R. 1983, *Absorption and Scattering of Light by Small Particles* (New York: Wiley).
Bouchet, P., Chalabaev, A., Danks, A., Encrenaz, T., Epchtein, N., and Le Bertre, T. 1987, *Astr. Ap.*, **174**, 288.
Bradley, J. P., Brownlee, D. E., and Fraundorf, P. 1984, *Science*, **223**, 56.
Bregman, J. D., Campins, H., Witteborn, F. C., Wooden, D. H., Rank, D. M., Allamandola, L. J., Cohen, M., and Tielens, A. G. G. M. 1987, *Astr. Ap.*, **187**, 616.
Brownlee, D. E. 1988, In *Infrared Observations of Comets Halley and Wilson and Properties of the Grains* (NASA CP-3004), p. 66.
Campins, H., and Ryan, E. V. 1988, *Ap. J.*, submitted.
Chyba, C., and Sagan, C. 1987, *Nature*, **330**, 350.
Combes, M., *et al.* 1986, *Nature*, **321**, 266.
Danks, A. C., Encrenaz, T., Bouchet, P., Le Bertre, T., and Chalabaev, A. 1987, *Astr. Ap.*, **184**, 329.
Eaton, N. 1984, *Vistas Astr.*, **27**, 111.
Gary, G. A., and O'Dell, C. R. 1974, *Icarus*, **23**, 519.
Gehrz, R. D., and Ney, E. P. 1986, in *Proc. 20th ESLAB Symposium* (ESA SP-250), **2**, 101.
Green, S. F., McDonnell, J. A. M., Pankiewicz, G. S. A., and Zarnecki, J. C. 1986, in *Proc. 20th ESLAB Symposium* (ESA SP-250), **2**, 81.
Güttler, A. 1952, *Ann. Physik*, **6**, 5.
Hanner, M. S. 1986, *Adv. Space. Res.*, **5**, 325.
———. 1988, in *Infrared Observations of Comets Halley and Wilson and Properties of the Grains* (NASA CP-3004), p. 22.
Hanner, M. S., Aitken, D. K., Knacke, R., McCorkle, S., Roche, P. F., and Tokunaga, A. T. 1985*a*, *Icarus*, **62**, 97.
Hanner, M. S., *et al.* 1985*b*, *Icarus*, **64**, 11.
Hanner, M. S., Tokunaga, A. T., Veeder, G. J., and A'Hearn, M. F. 1984, *A.J.*, **89**, 162.
Jessberger, E. K., Christoforidis, A., and Kissel, J. 1988, *Nature*, **332**, 691.
Kissel, J., *et al.* 1986, *Nature*, **321**, 336.
Knacke, R. F., Brooke, T. Y., and Joyce, R. R. 1986, *Ap. J.* (*Letters*), **310**, L49.
Krishna Swamy, K. S. 1986, *Physics of Comets* (Singapore: World).
Krishna Swamy, K. S., and Donn, B. 1968, *Ap. J.*, **153**, 291.
———. 1979, *A.J.*, **84**, 692.
Krishna Swamy, K. S., Sandford, S. A., Allamandola, L. J., Witteborn, F. C., and Bregman, J. D. 1988, *Icarus*, **75**, 351. (Paper I).
Krishna Swamy, K. S., and Shah, G. A. 1988, *M.N.R.A.S.*, in press.
Maas, R. W., Ney, E. P., and Woolf, N. J. 1970, *Ap. J.* (*Letters*), **160**, L101.
Mazets, E. P., *et al.* 1986*a*, *Nature*, **321**, 276.
———. 1986*b*, in *Proc. 20th ESLAB Symposium* (ESA SP-250), **2**, 3.
McKeegan, K. D., Walker, R. M., and Zinner, E. 1985, *Geochim. Cosmochim. Acta*, **49**, 1971.
Mukai, T., Mukai, S., and Kikuchi, S. 1986, in *Proc. 20th ESLAB Symposium* (ESA SP-250), **2**, 59.
Ney, E. P. 1974*a*, *Ap. J.* (*Letters*), **189**, L141.
———. 1974*b*, *Icarus*, **23**, 551.
———. 1982, in *Comets*, ed. L. L. Wilkening (Tucson: University of Arizona Press), p. 323.
Ney, E. P., and Merrill, K. M. 1976, *Science*, **194**, 1051.
Perry, C. H., Agrawal, D. K., Anastassakis, E., Lowndes, R. P., Rastogi, R. P., and Tornberg, N. E. 1972, *Moon*, **4**, 315.
Sandford, S. A. 1987, *Fund. Cosmic Phys.*, **12**, 1.
Sandford, S. A., and Walker, R. M. 1985, *Ap. J.*, **291**, 838.
Tokunaga, A. T., Golisch, W. F., Griep, D. M., Kaminski, C. D., and Hanner, M. S. 1986, *A.J.*, **92**, 1183.
Tokunaga, A. T., Nagata, T., and Smith, R. G. 1987, *Astr. Ap.*, **187**, 519.
van de Hulst, H. C. 1957, *Light Scattering by Small Particles* (New York: Wiley).
Wickramasinghe, D. T., and Allen, D. A. 1986, *Nature*, **323**, 44.
Wickramasinghe, D. T., Hoyle, F., Wickramasinghe, N. C., and Al-Mufti, S. 1986, *Earth, Moon and Planets*, **36**, 295.

L. J. ALLAMANDOLA, J. D. BREGMAN, K.S. KRISHNA SWAMY, SCOTT SANDFORD, and F. C. WITTEBORN: NASA/Ames Research Center, Mail Stop 245–6, Moffett Field, CA 94035